CHAPTER V

INFLUENCE OF OCEANIC INHOMOGENITIES ON SOUND PROPAGATION -SOME CASE STUDIES

5.1 INTRODUCTION

5.1.1 Oceanic inhomogenities and acoustics

In reality, the ocean is an extremely complex and variable medium. In such a complex environment more complex models of propagation incorporating statistical characteristics of the variations might be necessary to obtain reliable predictions of the sound field. Ocean currents, internal waves and small-scale turbulence perturb the horizontally stratified character of the sound speed and cause spatial and temporal fluctuations in sound propagation. Boundaries of large currents, such as the Gulf Stream and Kuroshio, represent frontal zones separating watermasses with essentially different characteristics. Within these frontal zones, temperature, salinity, density and sound speed suffer strong variations and hence the acoustic propagation (Levenson and Doblar,1976). Large eddies in the ocean are mostly observed near intense frontal currents. The parameters of synoptic eddies vary over rather wide range. The diameter of an eddy ranges from 25 to 500km. Analysis of propagation studies through a cyclonic Gulf Stream eddy revealed considerable variations in the propagation conditions (Vastano and Owens, 1973). Considerable fluctuations of the intensity and phase of sound waves arise in the presence of internal waves (Stanford,1974). We know that such characteristics of the

ocean water as salinity, temperature, density, and current velocity do not vary smoothly with depth, but in discontinuous fashion. Such fine layered structure leads to multipath of sound transmission and hence cause additional fluctuations of phase and amplitude to the sound signal (Stanford,1974). Thicknesses of these layers typically vary from tens of centimetres to tens of metres.

From the previous chapters it is inferred that the thermocline characteristics at deep and shallow regions in the Arabian Sea are influenced by a number of oceanographic phenomena namely meso-scale eddies, internal waves, upwelling, sinking, undercurrent etc. These processes result in the formation of various thermocline features such as step structures, sharp vertical gradient and bottom quasi-homogeneous layer with varying thermocline gradient and thickness. In association with the temporal and spatial variabilities in the thermocline one can expect fluctuations in the amplitude and phase of acoustic signals transmitted through the medium.

In the present study, some of the typical thermocline features identified from the previous chapters are used to delineate their role on acoustic propagation. A range-dependent numerical model is used for the simulation of propagation conditions.

5.1.2 DESCRIPTION OF THE MODEL

The basis of all the theoretical models of underwater sound propagation is the wave equation.

$$\nabla^2\phi = \frac{1}{c^2} \cdot \frac{\partial \phi^2}{\partial t^2}$$

where ∇^2 : Laplacian operator, ϕ :Velocity potential, c : speed of sound and t: time

The parabolic equation to the wave equation is of the form

$$\frac{\partial^2 p}{\partial z^2} + 2ik_o \frac{\partial p}{\partial r} + k_o^2(n^2 - 1)p = 0$$

where n : refraction index which is a function of depth(z), range(r) and azimuth(θ), p : pressure field (function of range and depth), k_o :reference wave number (ω/c_o), ω :source frequency and c_o : reference sound speed.

This equation is numerically solved by implicit finite difference technique (Lee and McDaniel,1988) which is a *marching solutions*. An advantage of this solution is that the calculation necessarily includes many receiver depths and is therefore the results are directly suitable for contouring.

The parabolic equation model (PE-IFD) is quite distinct from the other two main classes of models that are commonly used. The ray theoretical models are based on the assumption that acoustic wavelengths are small enough so that diffraction effects are negligible. The normal mode model is based on the approximation that the ocean is horizontally stratified so that coupling between the waveguide modes is negligible. The PE-IFD model retain these two so that it is valid to much lower frequencies and for more realistic, non-stratified oceans.

This model is used for computing acoustic propagation loss in both range-dependent and range-independent

environments. An important feature of this model is that it can handle arbitrary surface boundary conditions and an irregular bottom with arbitrary bottom boundary conditions. Another important feature of the model is that it can handle horizontal interfaces of layered media.

The inputs to the model are frequency (Hz), source depth (m), receiver depth (m) and range (m) as operational parameters. The environmental inputs are sound speed (m s^{-1}) profile, water depth (m), density (g/cc) atttenuation (dB/wave length) in the water and sediment layers. Reference sound speed and depth/range step sizes are the tuning factors of the model. The usual step sizes are one-fourth of a wave length and half wave length in depth and range respectively.

The model output is the transmission losses to the specified points in the depth-range plane. The model was implemented and validated using the transmission loss measurements made during an acoustic experiment off Cochin (Balasubramanian and Radhakrishnan, 1989;1990). They found good agreement between the experimental and simulations using the model.

The model described above is applied to simulate the propagation conditions under different oceanic environments. Several studies were carried out for the range-dependenet environments for other oceanic regions (Davis et al.,1982). The propagation under range-dependent scenario is not reported for Arabian Sea. This aspect is investigated using the PE-IFD model for a wide variety of oceanic features such as layered micro-structure, internal waves and eddy in the following sections.

To delineate the effect of the water born features, the influences of surface and bottom boundaries are kept minimum in the model. A pressure release sea surface is assumed so that the fields will vanish at the surface. An artificial absorbing bottom (Lee and Mc Daniel, 1988) was also assumed in the model to minimise the bottom effect.

5.2 THERMOCLINE AS AN ACOUSTIC BARRIER

As sound propagates, its energy gets refracted in water column depending on the prevalent sound speed gradients. Strong refractions and hence changes in the insonification pattern occur as the relative position of the source/receiver changes. In the ocean vertical gradient are more compared to horizontal. Most commonly large sound speed gradients occur in the thermocline region which in effect can act as a barrier for the sound energy propagating across it. For a given sound speed gradient in the thermocline, refraction increases with increase of the thickness of thermocline. Similarly, for a given thermocline thickness, higher the sound speed gradient higher the refraction. An important feature associated with this kind of refraction is the formation of shadow zones beneath the thermocline depth, which occur for a high frequency sound located near the sea surface.

The results in previous chapters indicate that the gradients and thickness of thermocline change drastically on climatic and synoptic time scales. The variations in gradient is of the order of $0.05^{\circ}C\ m^{-1}$ to $0.14^{\circ}C\ m^{-1}$ on climatic scale whereas it is of the order of $0.05^{\circ}C\ m^{-1}$ to $0.3^{\circ}C\ m^{-1}$ in the synoptic scale. Similarly, the thermocline thickness varies from 40 to 100m and 10 to 190m on synoptic and climatic scales respectively. Correspondingly, the

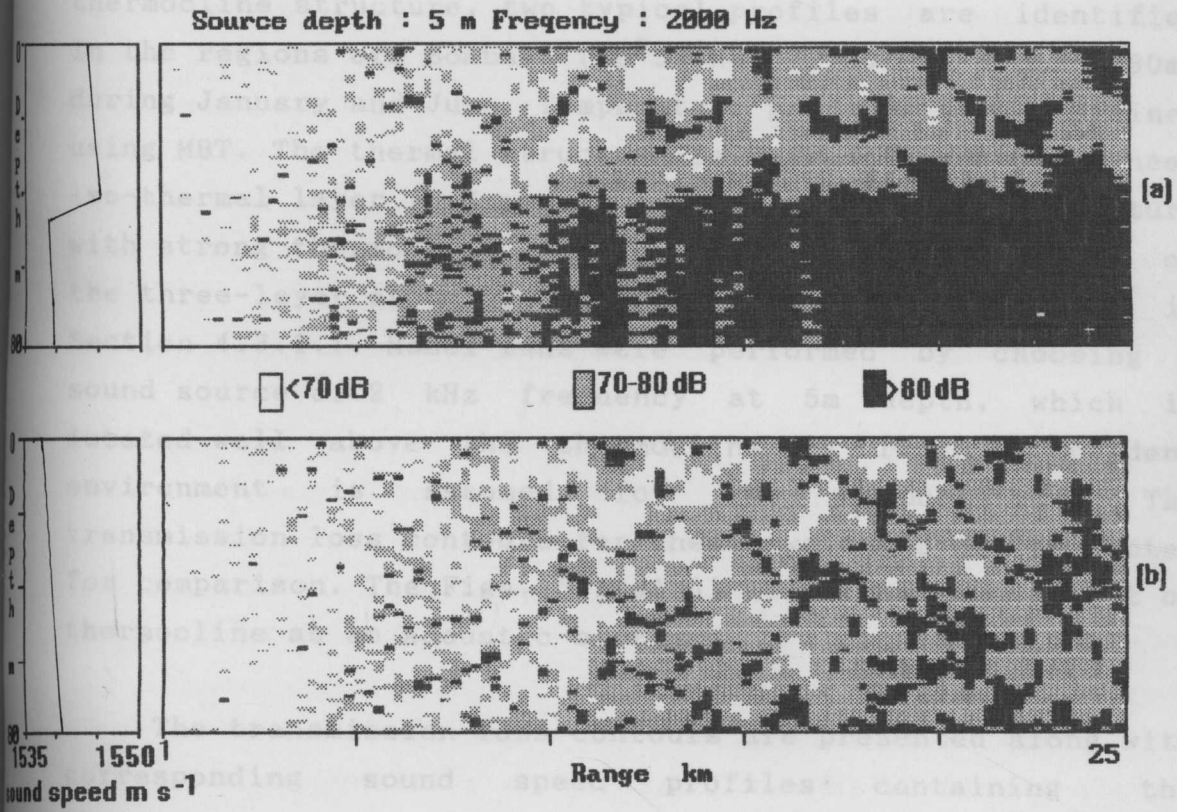

Fig.5.1 Iso-loss contours determined by PE-IFD model
(a) water column having thermocline
(b) water column having near iso-thermal condition

shadow zone variability also will be more.

5.2.1 MODEL SIMULATIONS OF TRANSMISSION LOSS

To simulate the sound propagation for different thermocline structure, two typical profiles are identified in the regions off Bombay (18°50'N, 71°35'E; depth <80m) during January and June. Temperature profiles were obtained using MBT. The thermal structure is characterised by a near iso-thermal layer in January and a three-layer structure with strong thermocline gradient in June. The formation of the three-layer structure in June is discussed in detail in Section 4.3.1.1. Model runs were performed by choosing a sound source of 2 kHz frequency at 5m depth, which is located well above the thermocline. A range-independent environment is assumed for the computations. The transmission loss contours for these two cases are presented for comparison. The Figs.(5.1(a&b)) illustrate the effect of thermocline as an acoustic barrier..

The transmission loss contours are presented along with corresponding sound speed profiles containing the three-layer structure (Fig.5.1a). The thermocline gradient is strong ($0.25^{\circ}C\ m^{-1}$) and found at a depth of 40m. The transmission loss contours show significant difference above and below the thermocline depth. The transmission loss increases slowly with range above thermocline depth, whereas it increases rapidly below it. This indicate that the energy below thermocline is very less compared to above it. Similarly, the profile without thermocline and corresponding transmission loss contours are presented in Fig.5.1b. Unlike the other case, this contours show that the transmission loss increases slowly with range for the entire water column. For instance, the 80dB contour found at a range of

11km below thermocline(70m), which is absent at same depth (where the loss is about 70dB) in the near isothermal case. This clearly indicates that the energy available below thermocline is very much limited for an acoustic source above thermocline. Moreover, a well marked shadow zone (transmission loss >80dB) is present below thermocline depth from 11km onwards, which is absent in the other case. The model runs were performed with the source below thermocline also indicated similar results. This suggests that thermocline act as an acoustic barrier for the passage of energy across it.

5.3 LAYERED OCEANIC MICROSTRUCTURE

Studies conducted by several authors indicate that the high frequency sound propagation is drastically affected by small scale oceanic features like inversions, step like structures, etc. (Melberg and Johannessen,1973; Ewart,1980; Unni and Kaufman,1983). This is mainly due to the fact that the inhomogeneities in the oceanic environment cause scattering and hence loss of energy for the transmitted signal. A recent study of Hareesh Kumar et al.(1995) clearly indicated the presence of step like structures in the thermocline in the Arabian Sea. The study also brought out sharp sound speed gradient associated with these step like structures.

During the 101th cruise of *FORV Sagar Sampada* fine scale measurements of temperature and salinity at close depth intervals (using Seabird CTD system; accuracy $\pm 0.001^{\circ}C$) were made in the coastal waters of Cochin ($9^{\circ}75'N;75^{\circ}75'E$) from 23 May to 3 June 1992. Vertical profiles of temperature and salinity are characterised by multiple subsurface maxima in salinity corresponding to the

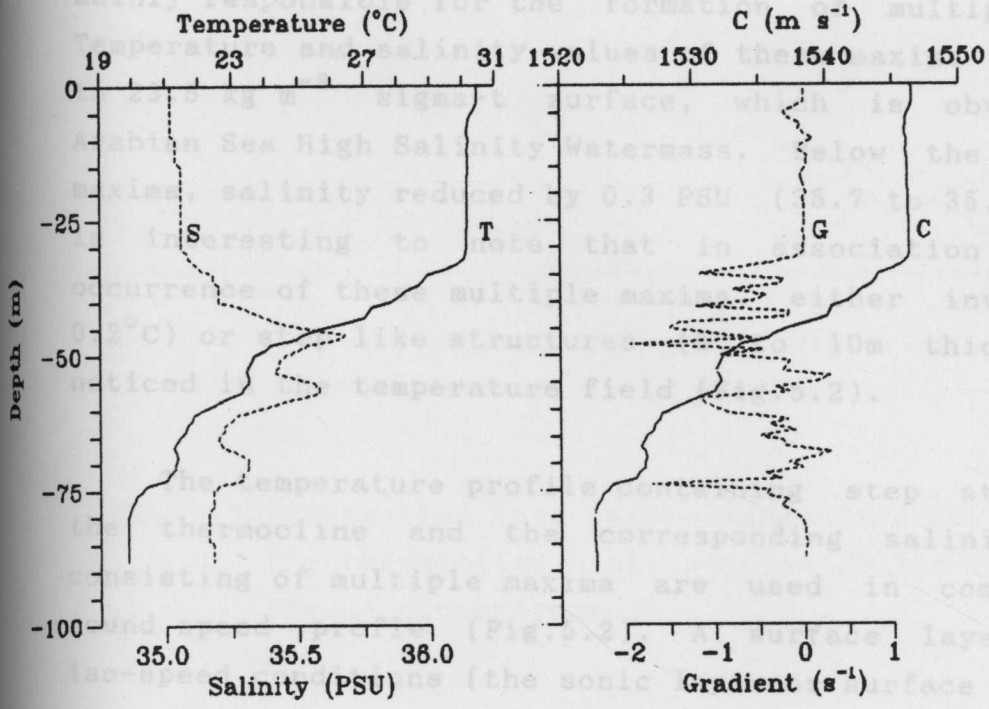

Fig.5.2 Vertical profiles of temperature, salinity, sound speed and sound speed gradient showing micro-structure in the thermocline.

thermocline region (Fig.5.2). These maxima are separated by pockets of low saline waters. Vertical separation between these multiple maxima varies from 10 to 15 m and their salinity progressively decreased with increasing depth. Among these, the upper maximum is more pronounced. The occurrence of the multiple maxima mostly coincided with the reversal of flow from southerly to northerly at 50m (Hareesh Kumar et al.,1995). Thus the prevailing flow pattern may be mainly responsible for the formation of multiple maxima. Temperature and salinity values of these maxima corresponds to 23.5 kg m^{-3} sigma-t surface, which is obviously the Arabian Sea High Salinity Watermass. Below the subsurface maxima, salinity reduced by 0.3 PSU (35.7 to 35.4 PSU). It is interesting to note that in association with the occurrence of these multiple maxima, either inversions ($\simeq$ 0.2°C) or step like structures (5 to 10m thickness) are noticed in the temperature field (Fig.5.2).

The temperature profile containing step structure in the thermocline and the corresponding salinity profile consisting of multiple maxima are used in computing the sound speed profle (Fig.5.2). A surface layer of near iso-speed conditions (the sonic layer or surface duct), of about 35 m is noticed. In the thermocline, sound speed varied from 1525 to 1546 m s^{-1}. The sound speed gradients (Fig.5.2) exhibited rapid fluctuations within the thermocline (-2 to 1 s^{-1}) caused by thermal inversions and multiple subsurface salinity maxima. The positive gradient in sound speed, caused by the advection of warm and low saline waters, coincided with the depths of multiple maxima.

5.3.1 MODEL SIMULATIONS OF TRANSMISSION LOSS

The influence of this layered micro-structure upon

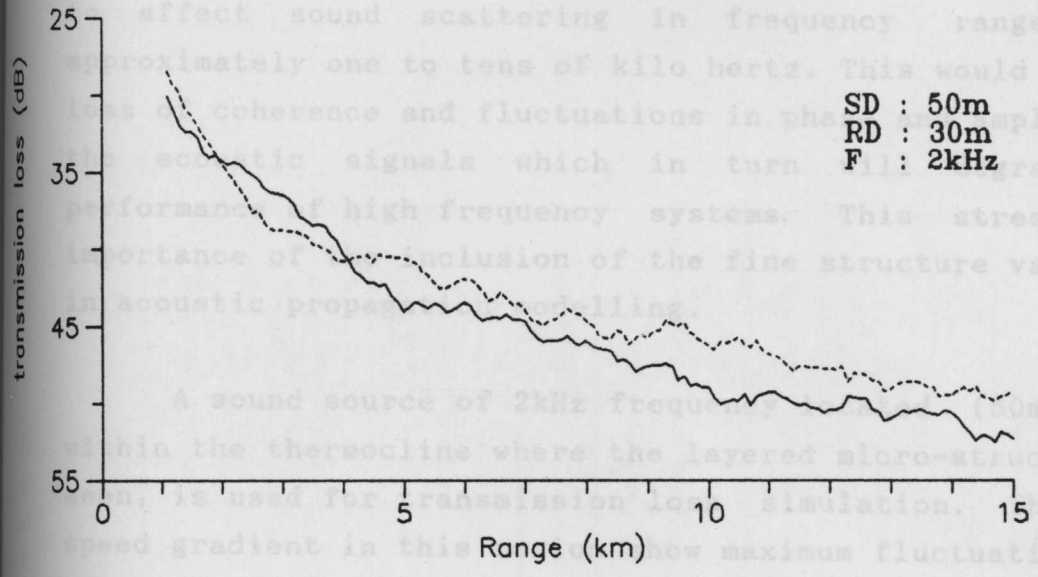

Fig.5.3 Propagation loss versus range from PE-IFD model for the thermocline with (continuous line) and without (dash) microstructure.

sound propagation is dependent on the sound speed gradients, the physical size and dynamics of the microstrucutre. As the vertical dimensions of the fine structures were of the order of 1 to 10m (Fig.5.2), their variability would be expected to affect sound scattering in frequency ranges from approximately one to tens of kilo hertz. This would lead to loss of coherence and fluctuations in phase and amplitude in the acoustic signals which in turn will degrade the performance of high frequency systems. This stresses the importance of the inclusion of the fine structure variations in acoustic propagation modelling.

A sound source of 2kHz frequency located (50m depth) within the thermocline where the layered micro-structure is seen, is used for transmission loss simulation. The sound speed gradient in this region show maximum fluctuations. The transmission loss values are simulated using the model. To delineate the effect of micro-structure, the transmission loss values are also simulated for the profile with smoothed microstrcture. The transmission loss with range (Fig.5.3) are presented for a receiver within the sonic layer (30m). This show the intensity fluctuation due to microstrcture in the thermocline. The transmission loss due to micro-structure in the thermocline is appreciably higher (2 to 4 dB)than the other case without micro-structure. However, for the ranges of 2km to 4km a reverse trend is noticed. This suggests the importance of fine structure in temperature and salinity on high frequency sound propagation.

5.4 INTERNAL WAVES

Previous studies indicated that the internal waves have got profound influence on acoustic propagation (Lee,1961;

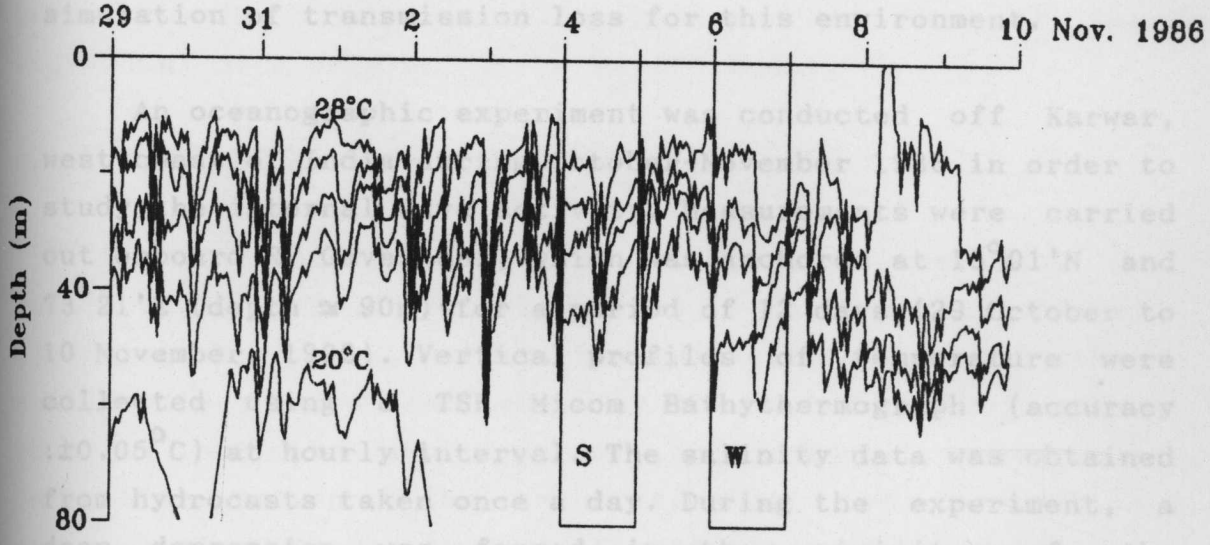

Fig.5.4a Passage of internal waves past a stationary observation point as evidenced by temporal fluctuations in isotherm patterns.

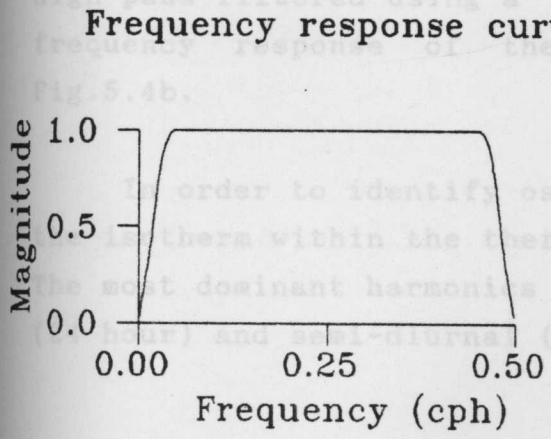

Fig.5.4b Freqency response curve of the Yulwalker digital filter design.

Porter et al.,1974; Baxter and Orr,1982; Murthy and Murthy,1986; Pinkel and Sherman,1991). This aspect was not studied for the Arabian Sea, though several studies (Varkey,1980; Murthy et al.,1992; Rao et al.,1995) reported the dominance of internal waves in this region. Hence, an attempt is made to analyse influence of internal waves on acoustic propagation based on observations and model simulation of transmission loss for this environment.

An oceanographic experiment was conducted off Karwar, west coast of India during October-November 1986 in order to study the internal wave activity. Measurements were carried out onboard RV Gaveshani, which was anchored at 15°01'N and 73°21'E (depth ≃ 90m) for a period of 12 days (29 October to 10 November, 1996). Vertical profiles of temperature were collected using a TSK Micom Bathythermograph (accuracy :±0.05°C) at hourly interval. The salinity data was obtained from hydrocasts taken once a day. During the experiment, a deep depression was formed in the vicinity of the observational point. Under the influence of this deep depression, the convergence induced at its periphery caused deepening of thermocline (Fig.5.4a). FFT analysis of temperature at different depth levels revealed low frequency harmonics (lower than inertial, ≃ 46 hrs), which was induced by the continuous deepening of the thermocline. To remove this low frequency component, the temperature data set is high pass filtered using a Yulwalker digital filter. The frequency response of the digital filter is shown in Fig.5.4b.

In order to identify oscillations in the thermocline, the isotherm within the thermocline are subjected to FFT. The most dominant harmonics are inertial (46 hour), diurnal (24 hour) and semi-diurnal (12 hour). The harmonics of the

inertial periodicity are generated by storm-induced wind field. Pollard (1970) also has observed inertial oscillations in connection with a sudden change of the wind speed and rapid changes in barometric pressure. In order to identify the influence of different harmonics on sound propagation, the entire data set is subjected to Yulwalker band pass filter. After having separated out the different harmonics, the model simulations were carried out for the individual data sets using the PE-IFD model.

5.4.1 MODEL SIMULATIONS OF TRANSMISSION LOSS

The internal wave spectrum occupies a continuum in scale; from the Brunt Vaisala period to the inertial period having all horizontal wavelengths and vertical wavelengths, possibly from a few centimetres to the depth of the ocean. To bring out the amplitude of the internal waves the depth-time section of the temperature at the observation point is shown in Fig.(5.4a). Fluctuations in temperature field is quite evident in the thermocline region and is due to internal wave propagation. In the absence of direct measurements, a two-layer approximation of the ocean was made for the computation of internal wave speed. Based on this approximation (Pond and Pickard, 1983) the speed (v), of the internal wave can be computed from

$$V^2 = gh\,[(\rho - \rho')/\rho']$$

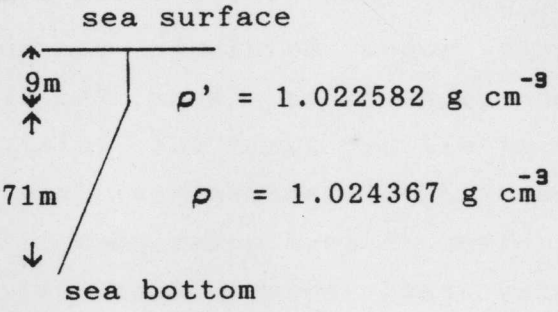

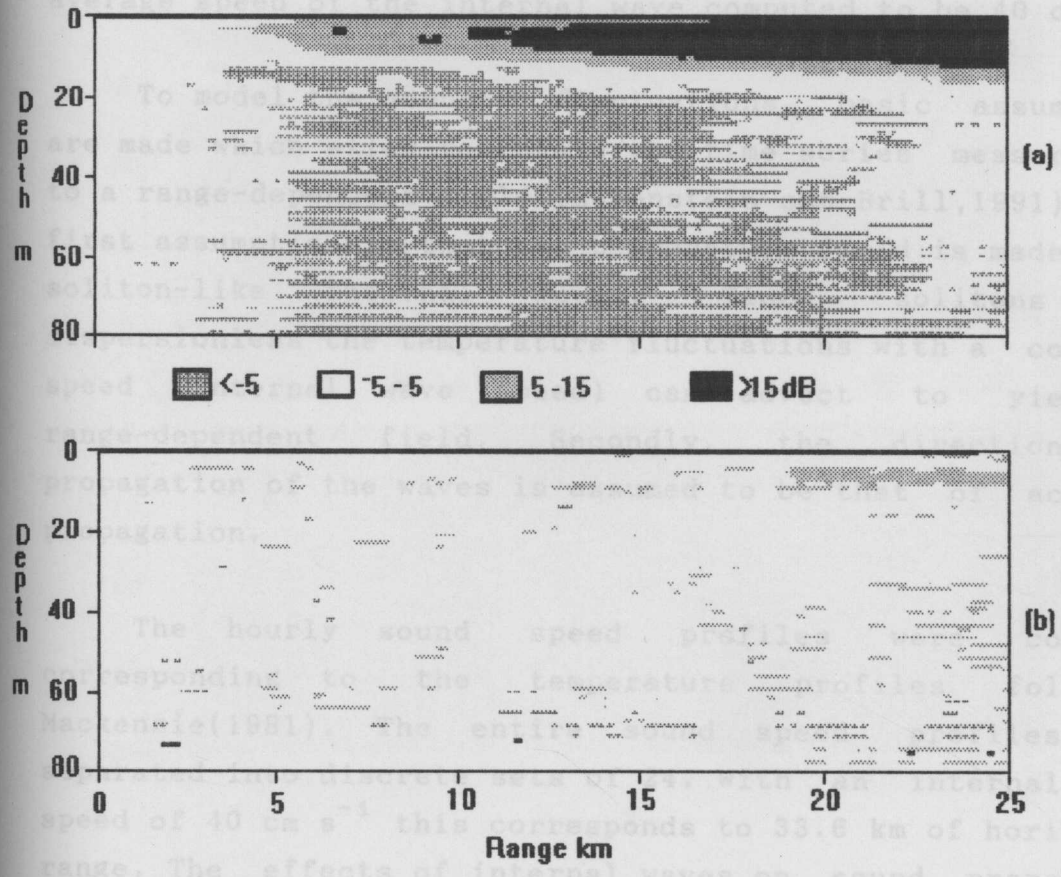

Fig.5.5 Intensity fluctuations due to internal wave fields (a) strong internal wave field (b) weak internal wave field

where g is the acceleration due to gravity, h is the thickness of the top layer of weak density gradient, ρ is the mean density of the bottom layer of strong density gradient, and ρ' is the mean density of the top layer. The average speed of the internal wave computed to be 40 cm s^{-1}.

To model the acoustic fluctuations, basic assumptions are made which allow to relate the time series measurements to a range-dependent field (Rubenstein and Brill,1991). The first assumption is that the temperature field is made up of soliton-like internal waves. Since solitons are dispersionless the temperature fluctuations with a constant speed (internal wave speed) can advect to yield a range-dependent field. Secondly, the direction of propagation of the waves is assumed to be that of acoustic propagation.

The hourly sound speed profiles were computed corresponding to the temperature profiles following Mackenzie(1981). The entire sound speed profiles are separated into discrete sets of 24. With an internal wave speed of 40 cm s^{-1} this corresponds to 33.6 km of horizontal range. The effects of internal waves on sound propagation is more in the frequency range 50Hz-20kHz (Etter,1991). A 3kHz source frequency source selected at 5m depth to simulate the transmission loss.

Acoustic intensity fields are simulated under range-dependent (with 24 profiles) and range-independent environments (with single profile). The first profile in the set of 24 is taken for the range-independent model simulation. The simulation of transmission loss is performed for all the sets. The array of transmission loss values

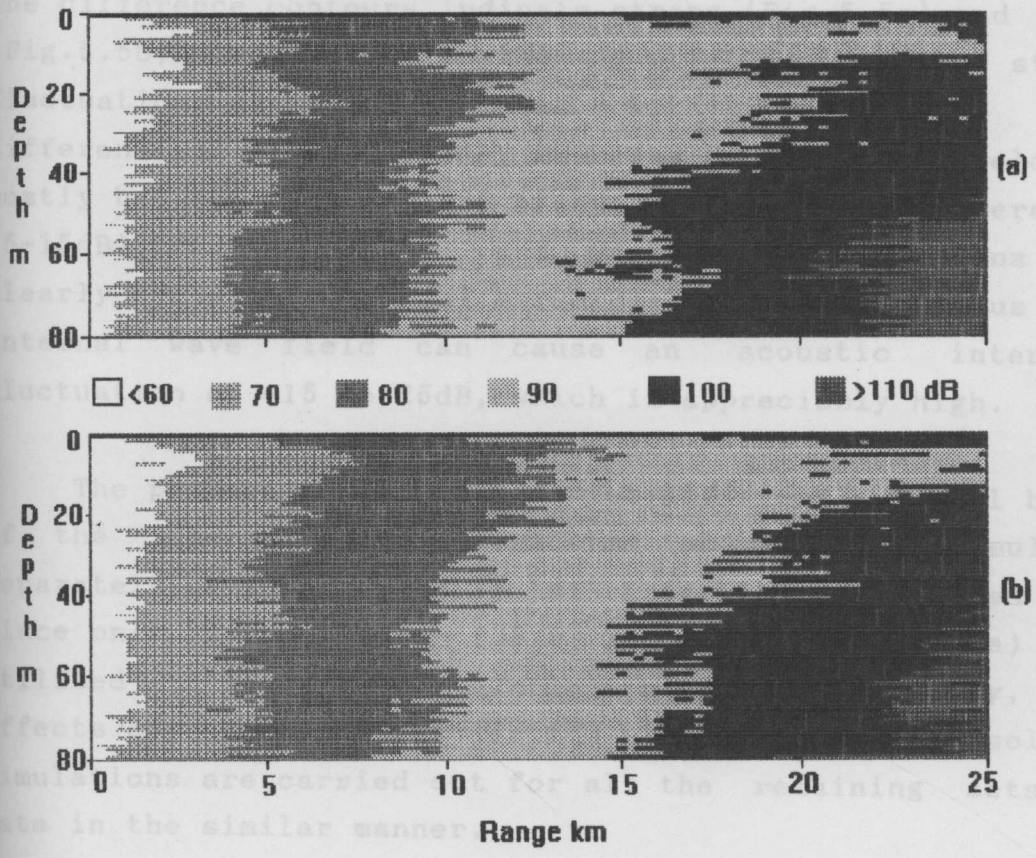

Fig.5.6 Contours of propagation loss as a function of range and depth for internal wave with (a) all the harmonics (b) high frequency harmonics (periods greater than 12hrs).

obtained from simulation for range-independent environment is subtracted from the corresponding array for the range-dependent environment to obtain a loss difference array. This difference array of transmission loss is contoured (difference contour) for all the individual sets. The difference contours indicate strong (Fig.5.5a) and weak (Fig.5.5b) fluctuations in the acoustic field. The strong fluctuations are associated with transmission loss difference of -15dB to 25dB, where as for the weak field it mostly between -5dB and 5dB except few higher differences (5-15dB).These strong (S) and weak (W) fluctuations are clearly evident in thermal structure (Fig.5.4a). Thus the internal wave field can cause an acoustic intensity fluctuation of -15 to 25dB, which is appreciably high.

The propagation conditions for different spectral bands of the internal waves mentioned above are simulated separately to identify their influence. It may be noted that since only 24 profiles (33.6 km horizontal range) are utilised for the present simulation spanning one day, the effects of inertial oscillation could not be resolved. Simulations are carried out for all the remaining sets of data in the similar manner.

The transmission loss contours for two sets viz., the set containing all the harmonics (Fig.5.6a) and for the higher frequency (higher than semi-diurnal) harmonics (Fig.5.6b) indicate that they are almost similar but with certain minor variations. To investigate further this aspect, the difference contours for two harmonics (diurnal and higher) are presented in Figs.(5.7(a & b)). The contours greater than 10dB difference are shaded black in the diagram. The difference field show large variations corresponding to the diurnal harmonics than the high

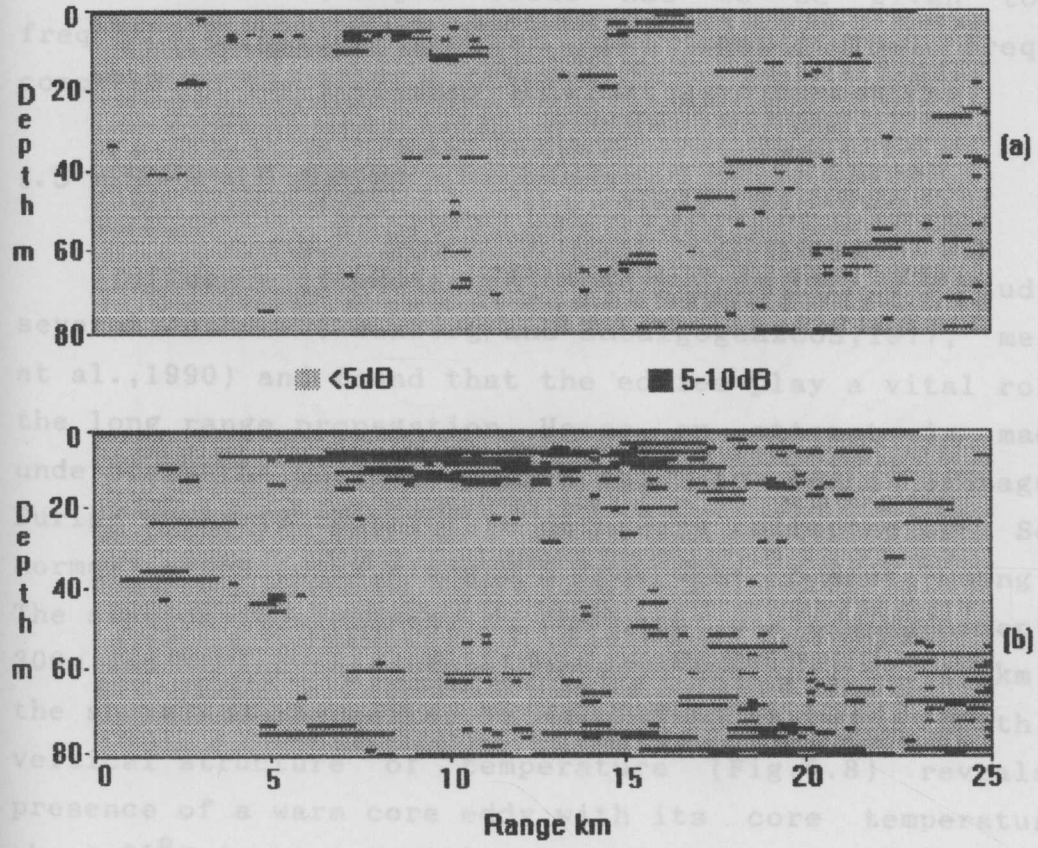

Fig.5.7 Difference contours of propagation loss values (a) high frequency harmonics (period greater than 12hrs) (b) diurnal frequency (period 24hrs)

frequency internal waves. This clearly suggest that the influence of high frequency harmonics closely resemble with internal wave field containing all harmonics. This established that to study the acoustic field in the presence of internal wave, major focus has to be given to high frequency harmonics (greater than semi-diurnal frequency) compared to low frequency internal wave harmonics.

5.5 MESO-SCALE EDDIES

Influence of eddies on sound propagation was studied by several authors (Weinberg and Zabalgogeazcoa,1977; mellberg at al.,1990) and found that the eddies play a vital role in the long range propagation. Hence, an attempt is made to understand the influence of an eddy on sound propagation. During MONEX-79 temperature data were collected off Somalia normal to the coast along 8°N from west to east using XBT. The station located near to the coast was having a depth of 300m and it increased to 4500m at a distance of 130km from the shore and thereafter it maintained the same depth. The vertical structure of temperature (Fig.5.8) reveals the presence of a warm core eddy with its core temperature of about 25°C (anticyclonic) which has an horizontal extent of approximately 600km and vertical extent of about 400m. The individual sound speed profiles across the eddy is presented in Fig.5.9. A sonic layer depth of about 220m is noticed corresponds to the trough of the eddy, where the sound speed is about 1531 cm s^{-1}. The sonic layer depths are vary from one end of the eddy to the other. Corresponding to this a sharp thermocline ($\cong$ 0.25°C m^{-1}) at a shallow depth ($\cong$ 20m) at the western periphery compared to a diffused ($<$ 0.06°C m^{-1}) and deeper ($\cong$ 40m) at the eastern side. However the core of the eddy is characterised by a deep thermocline ($\cong$ 220m) with a thermocline gradient of $\cong$ 0.1°C m^{-1}. Since the

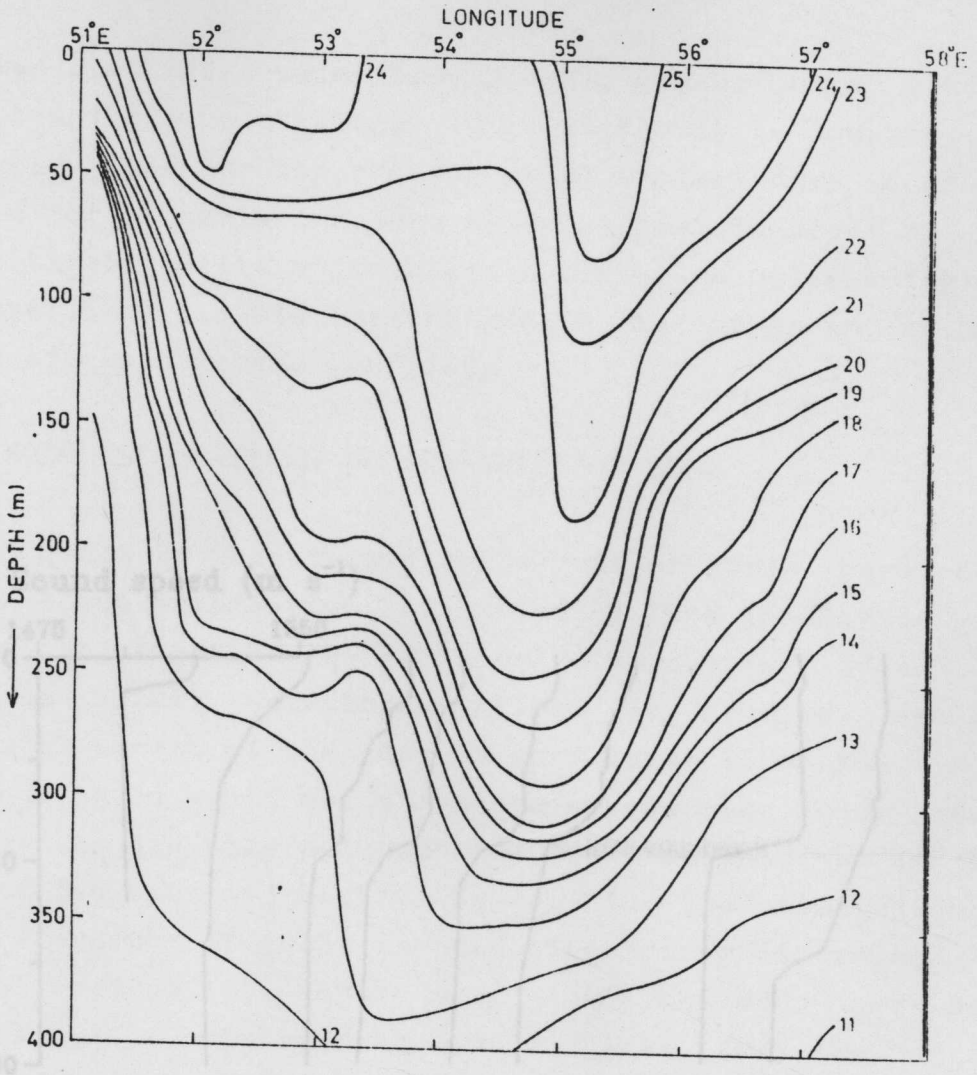

Fig.5.8 Presence of a warm core eddy evidenced by the spatial fluctuations in isotherm patterns.

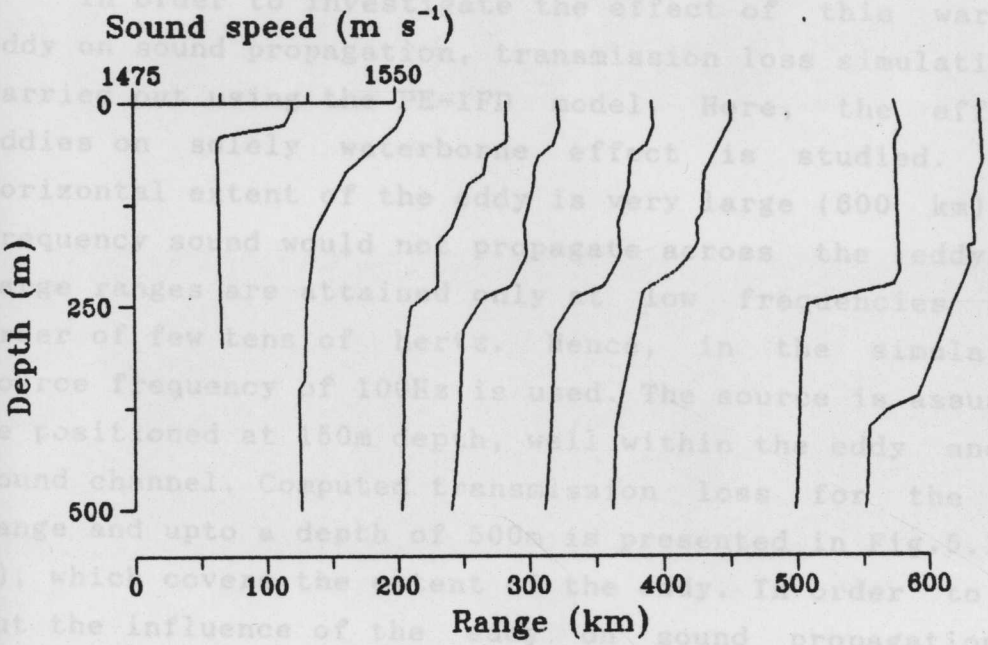

Fig.5.9 Vertical temperature profiles across the eddy

eddy was identified using hydrographic measurements without repeating the same stations, it is difficult to compute its movements. Thus for the present study a stationary eddy is assumed for transmission loss computations. In order to get the vertical profile up to station depth, a climatological mean profile available for the region is appended to the bottom of the observed profiles.

5.5.1 MODEL SIMULATIONS OF TRANSMISSION LOSS

In order to investigate the effect of this warm core eddy on sound propagation, transmission loss simulation were carried out using the PE-IFD model. Here, the effect of eddies on solely waterborne effect is studied. As the horizontal extent of the eddy is very large (600 km), high frequency sound would not propagate across the eddy. Such large ranges are attained only at low frequencies of the order of few tens of hertz. Hence, in the simulation a source frequency of 100Hz is used. The source is assumed to be positioned at 150m depth, well within the eddy and deep sound channel. Computed transmission loss for the entire range and upto a depth of 500m is presented in Fig.5.10(a & b), which covers the extent of the eddy. In order to bring out the influence of the eddy on sound propagation, the computations were repeated for an identical environment except that the water column is assumed laterally homogeneous. This is achieved by taking the initial sound speed profile to be representative of the entire range.

Transmission loss result obtained for both these cases are presented in Figs.5.10(a&b). Here, the shaded area represents regions with transmission loss higher than 100dB. The 100dB value was selected arbitrarily, such that all the convergence zones are represented in the figures. The

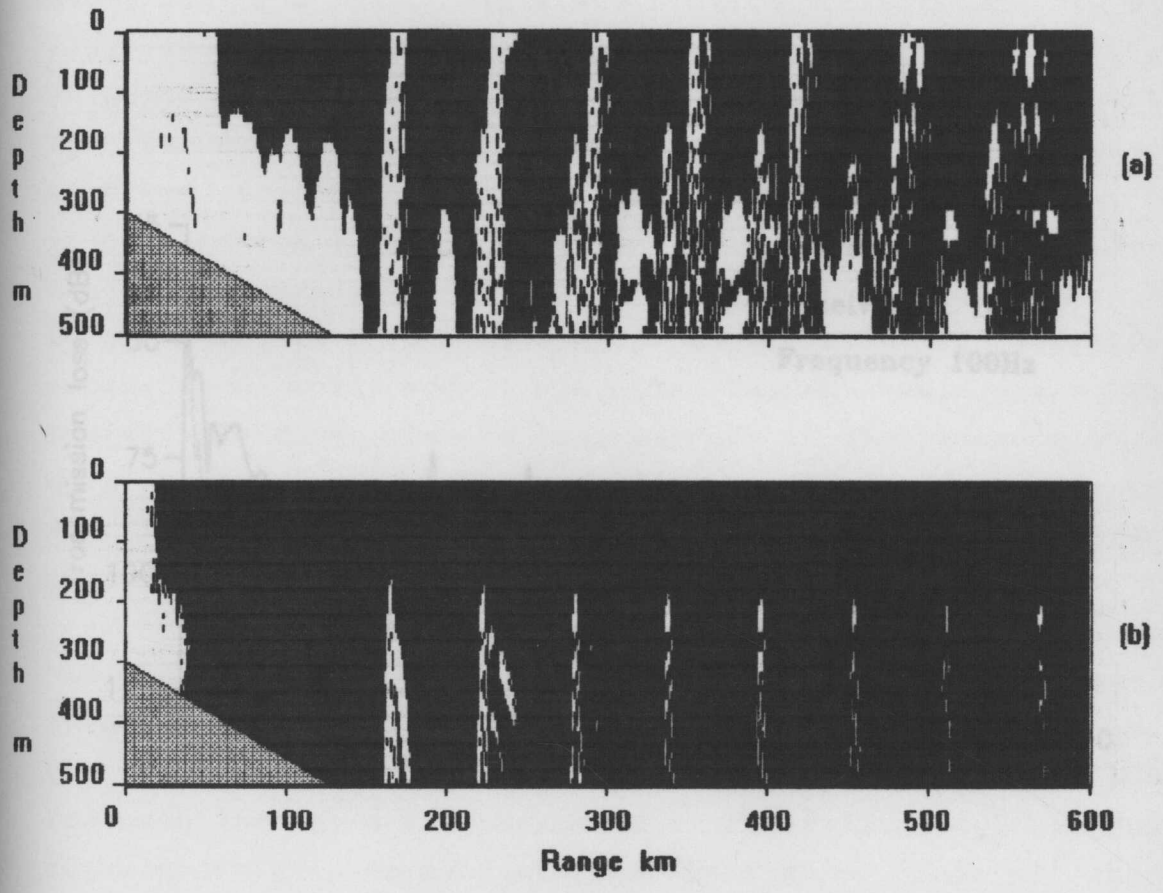

Fig.5.10 Iso-loss contours determined by PE-IFD model (a) propagation across the eddy (b) propagation without eddy. Shaded (black) area represent loss higher than 100 dB

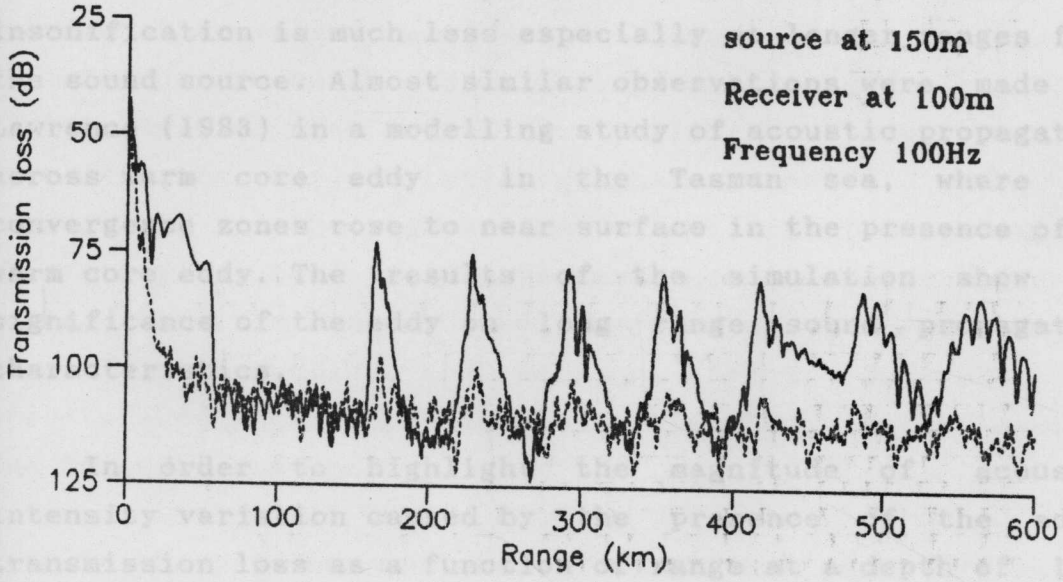

Fig.5.11 Propagation loss versus range from PE-IFD model for 100 Hz Frquency source at 150m depth and receiver at 100m depth. The Continous line for propagation across eddy and dash line for without eddy.

periodic narrow (10km wide at the surface) white vertical bands occurring in Fig.(5.10a) are the convergence zones which occur at a regular range interval of about 60km. The pattern is some what smeared as the depth increases but a high degree of insonification is evident at depths more than 250m. In contrast, Fig.5.10b, which corresponds to a range-independent, eddy-free environment does not show evidence of such convergence zones except at deeper levels than the source depth. The zones are well defined and sharp compared to the previous case. Also, the area of insonification is much less especially at longer ranges from the sound source. Almost similar observations were made by Lawrence (1983) in a modelling study of acoustic propagation across warm core eddy in the Tasman sea, where the convergence zones rose to near surface in the presence of a warm core eddy. The results of the simulation show the significance of the eddy on long range sound propagation characteristics.

In order to highlight the magnitude of acoustic intensity variation caused by the presence of the eddy, transmission loss as a function of range at a depth of 100m for both the cases are presented in Fig.5.11. About 15-20dB convergence gain is evident from the figure. Lateral shift in the pattern of the convergence zones of the order of about 10km is also noticed. The width of the convergence zone and lateral shift in the zone are all depend on the detailed nature of the eddy field.

CHAPTER VI

SUMMARY AND CONCLUSIONS

The present study has been undertaken with the objectives to understand the thermocline variability in the Arabian Sea and to investigate its influences on acoustic propagation. Though this type of study has been carried out for the other oceanic regions, the thermocline variability and associated acoustic propagation were not understood well for the Arabian Sea. One of the preliminary tasks was to identify the various oceanographic features that are responsible for the thermocline variability. The outcome of this study was that various factors such as eddies, internal waves, water masses, upwelling/sinking, undercurrents, summer/winter cooling and monsoon effects influence the structure of thermocline in the Arabian Sea, in the spatial and temporal domains.

In the present study major focus has been given to understand thermocline variability in the Arabian Sea as a whole. The typical parameters which are used to describe the thermocline characteristics are its top, thickness, gradient and oscillations. Subsequently to investigate the different processes prominent in the the coastal waters which have bearing on the thermocline characteristics, transects of temperature normal to the coast were analysed. The uniqueness of this data set is that several hydrographic sections were repeatedly made to cover the same stations. As the variabilities observed in the thermocline was found to be occurring on different time scales, the investigation was further extended to cover the short term aspects also. This

was achieved by analysing time series measurements made at several locations in the Arabian Sea. These data sets were collected for coastal as well as deep waters covering monsoon and non monsoon periods. After having described the thermocline variability, the propagation characteristics for different types of thermocline were investigated.

Climatological studies indicated that during pre-monsoon periods entire Arabian Sea was characterised by shallow thermocline (30-40m) due to surface heating. With the commencement of summer monsoon thermocline further shoaled in the the coastal regions due to upwelling. On the other hand deep thermoclines (>120 m) were noticed for the same period in the central Arabian Sea due to sinking and increased vertical mixing. One of the major findings is that strong spatial variability was noticed from July to September in the entire Arabian Sea. The scenario changed as the winter sets in. The thermocline was pushed down (>70m) in the coastal region. Thermocline thickness suggested that it is less than 40m in the northern Arabian Sea throughout the year. It increased (>100m) and average thermocline temperature drops to less than 20°C during summer monsoon. The thermocline gradient was found to be between 0.04°and 0.14°Cm^{-1}. Weak gradients are noticed in the northern Arabian Sea due to interaction of two different watermasses (Arabian Sea High Salinity and Persian Gulf watermasses). The decrease of gradient in the equatorial Arabian Sea from January to June is attributed to equatorial undercurrent which caused the spreading of isotherms in the thermocline.

Large variations in thermocline characteristics are noticed off the west coast of India on an annual cycle. Large cross shore and onshore dynamic processes were found to be responsible for the observed thermocline variability.

In response to these processes the thermocline was found to shoal and deepen along the entire west coast. One of the important findings of this study is that on an annual cycle the thermocline characteristics were found to exhibit a time lags from southern to northern locations.

Deep thermocline (>60m) is noticed off Ratnagiri from January to March. From May onwards the thermocline moved up due to upwelling and it almost surfaces (≅10m) during summer monsoon. The shallow thermocline is noticed even up to December. The thermocline gradient also increases during this period ($0.3^{o}C\ m^{-1}$ in October) which decrease to $0.08^{o}C\ m^{-1}$ in January. The influence of northward flowing undercurrent on thermocline variability was found to be negligible north of Ratnagiri.

Deep thermocline (>60m) is noticed off Kasargod from December to February. During pre-monsoon months it shoals to less than 25m due to accumulation of heat in the upper layers with very warm SST ($>30^{o}C$) associated with Indian Ocean warm pool. The thermocline during this period was thick (>190m) with weak vertical gradient ($0.075\ ^{o}Cm^{-1}$). With the progress of upwelling the gradient in the upper thermocline increases to over $0.2^{o}C\ m^{-1}$. However, in the lower thermocline the gradient was weak ($\cong 0.08^{o}C\ m^{-1}$). This is due to increased shear mixing associated with southerly surface currents and northerly undercurrent.

The deep thermocline observed during December-February shoals during pre-monsoon due to intense surface heating off Cochin. The upward movement of isotherms in the thermocline is evident from March and it surfaces by July/August, with strong vertical temperature gradient ($>0.2^{o}C\ m^{-1}$). Upwelling continues up to October. The down slopping of the isotherms

towards the coast in the lower thermocline is an indirect evidence of the presence of sub-surface northward undercurrent. As a result, in the lower thermocline weak temperature gradient ($0.03^{\circ}C\ m^{-1}$) are noticed due to strong shear mixing. The commencement of sinking results in the deepening of thermocline (>100m) in December. During this period the temperature gradient increased ($0.15^{\circ}Cm^{-1}$) which was an unique feature observed in this region.

Off Cape Comorin deep thermocline is observed (>70m) from December to January. Another important result that can be seen from vertical section of temperature was the occurrence of a clockwise eddy (warm core) centered about 150 km from the coast. The core temperature of the eddy was found to be 27°C and its radius about 50 km. At the centre of the eddy thermocline was deeper by about 50m compared to its peripheries. The thermocline surfaces by July/August due to upwelling as off Cochin and Kasargod. During major part of the year upwelling dominated (March-October) compared to sinking (November-February) process.

The analysis further revealed that surfacing of thermocline leads to significant cooling in the surface layers (≅6°C off Cape and Cochin, 4°C off Kasargod). However, the thermocline did not surface off Ratnagiri. The downward movement of thermocline (sinking) starts by October, October-November, November and January off Cape, Cochin, Kasargod and Ratnagiri respectively. Thus it was observed that there was a time lag of about a month for the commencement of sinking process from south to north.

The average temperature decreases sharply at all locations due to upwelling compared to periods of sinking. The annual range of average temperature of thermocline is

maximum off Cochin (5°C) and minimum (3°C) off Ratnagiri. Average rate (per month) of upward movement of isotherms was found to be 30m, 23m, 29m and 11m off Cape, Cochin, Kasargod and Ratnagiri respectively, suggesting stronger upwelling off the south west coast of India. The deepening rate isotherm was found to be about 2 to 5 times faster during the period of sinking, compared to that of upwelling.

The T-S analysis indicated the presence of Arabian Sea high salinity watermass in the thermocline throughout the year. However, the effect of Bay of Bengal watermass was marginal in the thermocline. The low saline equatorial Indian Ocean watermass is also evident in the thermocline.

The average temperature of thermocline indicated drastic cooling from pre-monsoon to monsoon. The cooling is found to be maximum south of 14°N and north of 20°N. The strong upwelling off the south west coast of India and winter cooling north of 20°N coupled with pre-monsoon heating induced large annual ranges in thermocline temperature (≅10°C).

The analysis of short-term variability of thermocline at selected locations in the Arabian Sea brought out several interesting features. A three-layer vertical temperature profile with strong thermocline (2.5°C in 10m) was observed off Bombay in June/July, whereas much weaker thermoclines were observed in the central Arabian Sea. This strong thermocline off Bombay was the result of intense pre-monsoon heating followed by vertical mixing in the upper 50m (due to monsoon activity) over the remenant of winter water. The dynamic aspects of three layer structure investigated with the help of Richardson number indicated high values (7.4 in thermocline) off Bombay. This is an evidence of the

suppression of turbulence which enabled the three layer structure with strong thermocline gradient to be maintained throughout the period of observation. Further the thickness of the thermocline was only 10m at this location.

The thermocline was shallower off Karwar in September (5m) compared to June (20m) mainly due to the effect of upwelling. The thermocline gradient also showed a higher value of 0.3°C m^{-1} in September compared to January (0.15 °C m^{-1}. Another note worthy feature at this location was the presence of bottom isothermal layer. The spectral characteristics indicated that oscillations of inertial, diurnal and semi-diurnal periodicity occur in the thermocline.

The effect of upwelling on thermocline characteristics is clearly evident in the temperature profiles off Cochin. The thermocline shoaled and the isotherms moved up between April and June. The temperature at 60m dropped by as much as 6°C during this period. The 25°C isotherm moved up at an average speed of 1.1 m day^{-1} and thermocline gradient also doubled (0.1 to 0.2 °C m^{-1}) during this period. The vertical current shear increased from 0.005 s^{-1} to 0.25 s^{-1} from April to June showing increased turbulence in the lower thermocline. This suggested increased mixing in the thermocline due to southerly surface flow and northerly undercurrent in June. The Richardson number decreased from 0.2 to 0.05 during this period suggesting dynamic instability.

The thermocline variations on short time scales differed markedly in the deep stations compared to coastal stations. In the eastern Arabian Sea intense surface heating produced a shallow thermocline (≅20m) during pre-monsoon.

With the progress of the monsoon though thermocline deepens to 100m the isotherms within it moved up. This resulted in the increase of thermocline gradient (<0.1 to >0.02 $^{o}C\ m^{-1}$).

Oceanographic aspects of thermolcine characteristics for the Arabian Sea indicated that large variabilities in both spatial and temporal domains exist. In association with these variabilities one can expect large variations in the acoustic propagation characteristics also. This is due to the fact that temperature is one of the important parameters determining sound speed in the ocean. This clearly indicate that *apriori* knowledge of thermocline characteristics is very much essential to understand the propagation conditions in the sea. Transmission loss and sound speed are the two important parameters which are commonly used to describe the propagation conditions in the ocean medium.

Simulation of transmission loss carried out with the help of a range dependent model (PE-IFD) for different features associated with thermocline indicated that each of them affect propagation in a distinct manner. As the thermocline acts as a barrier for the passage of acoustic energy from either side, occurrence of shadow zones are associated with its characteristics. Shadow zones, the regions of weak sound intensity, were found to exhibit large variations depending on the thermocline gradient and thickness. When thermocline gradients were sharp it was found that a prominent shadow zone occurred at near ranges and vice versa. Sharp gradients in thermocline were generally found to exist during the periods of upwelling in the coastal Arabian Sea. Thus one can expect prominent shadow zones during this period.

Numerical experiments carried out with different

thermocline features indicated large fluctuations in the intensity of acoustic energy. Typical case studies were carried out to simulate the propagation conditions for oceanic layered microstructure, internal waves, meso-scale eddy field.

The results indicated that inclusion of layered microstucture in the propagation model is important as it was found to influence intensity fluctuation in the acoustic field. A deference (with and without microstructuree) of 2-4 dB transmission loss was found to exist for a source of 2 kHz frequency when the layer thickness was ≅10m. The oscillations associated with thermocline (internal waves) are found to influence propagation to a large extent. In the presence of weak internal wave activities (identified from thermal structure) the transmission loss fluctuation was found to be -5 to 5 dB. On the contrary, it was -15 to >20 dB for strong internal wave field. This clearly establishes that internal waves can cause large fluctuations (3 to 4 times) in the acoustic intensity. Further, influence of different harmonics on sound propagation suggested that periods higher than the semi-diurnal (12 hrs) were predominant compared to low frequencies. This also establish major focus has to be given to high frequency harmonics compared to low frequency harmonics. Simulations carried out for a warm core eddy with a source of 100Hz frequency at 150m depth revealed that convergent zones are found to extend to the surface. This suggest that more energy would be available in the near surface region compared to a situation where eddy is absent. Moreover the area of insonifications is found to be much less and sharp in the absence of an eddy field and vice versa. Another important result is that there was a convergence gain of 15-20 dB at 100m depth in presence of eddy. A lateral shift of about

10km was noticed in this pattern at this depth.

FUTURE OUTLOOK

In the present study the problem of thermocline variability in the Arabian Sea has been addressed in terms of various oceanographic factors and their influence on acoustic propagation. Though a number of oceanographic factors could be identified from the data sets used, specific data collection programme need to be planned to address the thermocline aspects in greater detail. In this programme the aspects like layered microstructure, directional internal waves, eddies, currents etc need to be monitored for basin wide at close spatial and temporal resolutions. However, the tremendous logistics involved for carrying out such a programme prevented us from taking up this task. Systematic observations of thermocline with relevent data on various physical processes would enable to develop a numerical model of the thermocline.

The study could be further extended using the fine scale measurements to study more realistic transmission loss characteristics which can be used as a back ground to asses the propagation conditions. The transmission loss studies carried out in the frame work of a range dependent model need to be validated with proper experimental data. This would improve the capability of underwater surveillance.

REFERENCES

Ali H B (1993) Oceanographic variability in shallow water acoustic and the dual role of the bottom. *IEEE Journal of oceanic engineering*, 18,(1) 31-41.

Antony M K (1990) Northward undercurrent along the west coast of India during upwelling - Some inferences. *Indian Journal of Marine Sciences*, 19, 95-101.

Baer R N (1981) Propagation through a three dimensional eddy including the effect on an array. *Journal of Acoustical Society of America*, 69, 70-75.

Balasubramanian P and K G Radhakrishnan (1989). Implementation of a range dependent transmission loss model based on Parabolic equation method. *Departmental report No.RR*-13/89, Naval Physical and Oceanographic Laboratory, Kochi.pp25.

Balasubramanian P and K G Radhakrishnan (1990) PE:IFD model versus off Cochin experimental data *Journal of Acoustical Society of India,* XVIII, 78-82.

Banse K (1968) Hydrography of the Arabian Sea shelf of India and Pakistan and effects on demersal fishes. *Deep-Sea Research*, 15, 45-79.

Bauer S, G L Hitcock and D B Olson (1991) Influence of monsoonally forced Ekman dynamics upon surface layer depth and plankton biomass distribution in the Arabian Sea. *Deep Sea Research*, 38, 531-553.

Baxter L,II and M H Orr (1982) Fluctuations in Sound transmission through internal waves associated with the thermocline: A computer model for acoustic transmission through sound velocity fields calculated from thermistor chain, CTD,XBT,and acoustic backscattering. *Journal of Acoustical Society of America* 71(1) 61-66.

Beckerle J, Baxter L, Porter R, Spindel R(1980) Sound channel propagation through eddies South West Off the Gulf Stream. *Journal of Acoustical Society of America* 68 : 1750-1767

Brekhovskikh L and Lysanov Yu (1982) *Fundamentals of ocean Acoustics* springer-Verlag, Berlin Heidabbery- pp250.

Brock J C, C R McClain, M E Luther and WW Hay (1991) The phytoplankton bloom in the northwestern Arabian Sea during the southwest monsoon of 1979. *Journal of Geophysical Research*, 96, 20613-20622.

Brock J C, C R McClain and W W Hay (1992) A Southwest monsoon hydrographic climatology for the Northwestern Arabian sea. *Journal of Geophysical Research* 97 (C0) 9455-9465.

Bruce J G (1974) Some details of upwelling off the Somali and Arabian coasts. *Journal of Marine Research*, 32, 419-423.

Bruce J C, Quadfasel D R, Swallow J C (1980) Somali eddy formation during the commencement of the South West monsoon of 1978. *Journal of Geophysical Research* 85 (C11): 6654-6660.

Charyulu R J, Y V B Sarma, M S S Sarma and L V G Rao (1994) Temperature oscillations in the upper thermocline region - A case of internal wave off Kalpeni island in the southern Arabian Sea. *Indian Journal of Marine Sciences*, 23, 14-17.

Chen CT, and F J Millero(1977) Speed of sound in sea water at high pressures. *Journal of Acoustical Society of America*. 62, 1129-1135.

Clark J G and M Kronengold (1974) Long period fluctuations of CW signals in deep and shallow water *Journal of Acoustical Society of America*, 56,1071-1083.

Colborn J G (1975) The thermal structure of the Indian Ocean. University Press of Hawaii, Honolulu, pp173.

Colosi J A, S M Flatte and C Bracher (1994) Internal wave effects on 1000 km oceanic acoustic pulse propagation, simulation and comparison with experiment. *Journal of Acoustical Society of America*, 96, 452-468.

Currie R I, A E Fisher and P M Hargreaves (1973) Arabian Sea upwelling. In : The biology of the Indian Ocean, B Zeitzchel and S A Gerlach (Ed.),Springer-Verlag, 37-53.

Cutler A and J Swallow (1984) Surface currents of the Indian Ocean (to 25°S,100°E) (Compiled from Achieved historical data). (UK Institute of Oceanographic Sciences, Bracknell) pp 8 and charts 36. 36.

Das V K Gouveia A D, Varma K K (1980) Circulation of Water characteristics on isanosteric surfaces in the Nothern Arabian Sea during February -April.*Indian journal of Marine Science* 9(3) 156-165.

Davis J A , White D and Cavanagh R C,(1982) Norda parabolic equation workshop, 31 March- 3 April 1981. *Naval Ocean Research and Development Activity, Technical Note* pp143.

Darbyshire M (1967) The surface waters off the coast of Kerala, southwest India. *Deep-Sea Research*, 14, 295-320.

Defant (1936) Die troposphare des Atlantaschen Ozeans. Schichtung und Zirkulation des Atlantischen Ozeans. Deutsche Atlantische Expedition "Meteor" 1925-1927 Wissenschaaftl . Erg;6(1): pp289.

Del Grosso V A (1974) New equation for the speed in natural water (with comparison to other equations), *Journal of Acoustical Society of America* 56, 1084.

Del Grosso, V A and C W Mader (1972) Speed of sound in sea water samples. *Journal of Acoustical Society of America.* 52 961-974

Desaubies Y J F (1976) Acoustic phase fluctuations induced by internal waves in the Ocean. *Journal of Acoustical Society of America* 60(4) 795-799

Desaubies Y J F (1978) On the scattering of sound by internal waves in the ocean. *Journal of Acoustical Society of America*, 64, 1461-1469.

Duing W (1972) The structure of sea surface temperature in monsoonal areas. In : Studies in Physical Oceanography, A L Gordon (Ed.) 1-18.

Duing W and A Leetmaa (1980) Arabian Sea cooling : A preliminary Heat Budget. *Journal of Physical Oceanography*, **10**, 307-312.

Elliot A J and G Savidge (1990) Some features of the upwelling off Oman. *Journal of Marine Research*, **48**, 319-333.

Etter P C (1991) Underwater Acoustic Modeling : Principles, techniques and applications. **Elseiver Applied Science, New York** pp297.

Ewart T E (1980) A Numerical simulations of the effects of Oceanic Fine structure on the acoustic transmission, *Journal of Acoustical Society of America*, **67(2)**, 496-503.

Flatte S M, Dashen R, W H Munk, K M Waston and F Zachariasen (1979) Sound transmission through a fluctuating Ocean. **Cambridge University Press, Cambridge UK** ,85-161.

Flatte S M and F D Tappert (1975) Calculation of the effect of internal waves on oceanic sound transmission. *Journal of Acoustical Society of America*, **58**, 1151-1159.

Gallagher J F (1966) The variability of watermasses in the Indian Ocean. **Publication National Oceanographic Data Centre**, G-11, 1-74.

Hamilton G R (1974) The variations of sound speed over long paths in the Ocean :International workshop on low frequency propagation and noise, Woods Hole, M.A. 7-30.

Hareesh Kumar P V (1994) Thermohaline variability in the upper layers of the Arabian Sea, Ph.D thesis, Cochin University of Science and Technology, pp108.

Hareesh Kumar P V and N Mohan Kumar (1995) On the flow and thermohaline structure off Cochin during the pre-monsoon season, Continental Shelf Research (in press).

Hareesh Kumar P V, N Mohan Kumar and K G Radhakrishnan (1995) Multiple subsurface maxima in vertical salinity structure - A case study. *Indian Journal of Marine Sciences*, 24, 77-81.

Hart T J and R I Currie (1960) The Benguela Current. *Discovery Report*, 8, 437-457.457.

Hastenrath S and L Grieschar (1989) Climatic Atlas of the Indian Ocean - Part III : Upper - ocean structure. (University of Winsconsin press,Madison) pp247.

Hastenrath S and P Lamb (1979) Climatic Atlas of the Indian Ocean - Part I : Surface Climate and Atmospheric circulation (Wisconsin University Press Madison, p 11 and Figs 97.

Hasternath S and J Merle (1987) Annual cycle of subsurface thermal structure in the tropical Atlantic Ocean. *Journal of Physical Oceanography*, 17, 1518-1538.

Henrick R F (1980) General effects of currents and sound speed variations on short range acoustic transmission in cyclonic eddies. *Journal of Acoustical Society of America* 67 No:1 121-134.

Itzikowitz S, M J Jacobson and W L Stiegmann (1982) Short range acoustic transmission through cyclonic eddies between a submerged source and receiver. *Journal of Acoustical Society of America*, 71, 1131.

Johannessen O M, G Subbaraju and J Blindheim (1981) Seasonal variation of the oceanographic conditions off the southwest coast of India during 1971-75. *FiskeriDir. Skr. Ser.*, 18, 247-261.

Joseph M G, P V Hareesh Kumar and B Mathew (1990) Short term pre-onset southwest monsoonal transformations in upper western equatorial Indian Ocean. *Indian Journal of Marine Sciences*, 19, 251-256.

KNMI, (1952), Indische Ocean Oceanographische and Meteorologische gevens., 2Ed. Publ. No. 135, pp (31) and 24 Charts.

Krishnamurti T N (1981) Cooling of the Arabian Sea and the onset vortex during 1979 In: Recent Progress in equatorial oceanography, Report of final meeting of SCOR Working Group 47 Venice, Italy.

Lawarence M W (1983) Modeling of acoustic propagation across warm core eddies. *Journal of Acoustical Society of America.* Vol 73(2), 427-485.

Lee D and S T Daniel (1988) Ocean Acoustic Propagation by finite difference methods. Pergamon Press New York, pp423.

Lee O S (1961) Effect of an internal wave on sound in the ocean. *Journal of Acoustical Society of America*, 33, 677-681.

Leetmaa A and H Stommel (1980) Equatorial current observations in the western Indian Ocean in 1975 and 1976. *Journal of Physical Oceanography*, 10, 258-269.

Leetmaa A, D R Quadfasel and D Wilson (1982) Development of the flow field during the onset of the Somali Current,1979. *Journal of Physical Oceanography*, 12, 1325-1342.

Leipper D F (1967) Observed ocean conditions and hurricane Hilda, 1964. *Journal of Atmospheric Science*, 24, 182-196.

Levenson, C and R A Doblar (1976) Long range acoustic propagation in the Gulf Stream. *Journal of Acousical Society of America.* 59, 1134.

Levitus S (1982) Climatological Atlas of the world ocean. (US Government Printing Office, Washington DC) pp213

Mackenzie K V (1981) Nine-term equation for sound speed in the Oceans. *Journal of Acoustical Society of America.* 70, 807.

Medwin H (1975) Speed of sound in water : A simple equation for realistic parameters. *Journal of Acoustical Society of America* 58, 1318

Mathew B (1981) Studies on upwelling and sinking in the seas around India, Ph.D Thesis, University of Cochin pp159.

McCreary J and P K Kundu (1989) A numerical Investigation of Sea Surface Temperature Variability in the Arabian Sea. *Journal of Geophysical Research*, 94, 16097-16114.

Mellberg L E, A R Robinson and G Bostew (1990) Modeled time variability of acoustic propagation through a Gulf stream meander and eddies. *Journal of Acoustical Society of America*, 87, 1044-1053.

Mellberg L E and O M Johanessen (1973) Layered oceanic microstructure - its effect on sound propagation. *Journal of Acoustical Society of America*, 53, 571-580.

Miles J W (1961) On the stability of heterogeneous shear flows. *Journal of Fluid Mechanics*, 10, 496-508.

Mohan Kumar N (1991) A study on air-sea interaction processes over the Indian Seas, Ph.D thesis, Indian Institute of Technology, Delhi. pp132.

Mohan Kumar N, P V Hareesh Kumar and M X Joseph (1995) Response of the coastal waters off Karwar to summer monsoonal forcing during 1989. *Continental Shelf Research*, 15, 883-888.

Mohanty U C, Dubey, S K and Singh M P (1983) A study of heat and mositure budget over the Arabian Sea and their role in the onset of maintenance of summer monsoon. *Journal of Meteorological Society of Japan*, 61, 208-221.

Molinari R L (1983) Somali Basin response to the monsoon and the feed back effect of the atmosphere. (CCCO Panel on Indian Ocean Climatic Studies, First Session,Paris)

Molinari R L, J F Festa and J C Swallow (1986a) Mixed layer and thermocline climatologies in the western Indian Ocean (Atlantic Oceanographic and Meteorological Laboratory, Miami), pp40.

Molinari R L, J C Swallow and J F Festa (1986b) Evolution of near surface thermal structure in the western Indian Ocean during FGGE 1979. *Journal of Marine Research*, 44, 739-763.

Montgomery R B and Stroup E D (1962) Equatorial waters and currents at 150°W in July-August 1952. Johns Hopk Oceanogr. studies, 1-68.

Munk W H (1980) Horizontal deflections of acoustic fronts by mesoscale eddies. *Journal of Physical oceanography* 10, 596-604.

Munk W H and Zachariasen (1976) Sound propagation through a fluctuating ocean theory and observation. *Journal of Acoustical Society of America*, 59, 818-838.

Muraleedharan P M, M R Ramesh Kumar and L V G Rao (1995) A note on poleward undercurrent along the southwest coast of India. *Continental Shelf Research*, 15, 165-184.

Murthy P G K and G R K Murthy (1986) A case study on the influence of internal waves on sound propagation in the sea. *Journal of Sound and Vibration*, 108, 447-454.

Murthy P G K, G S Sharma, V V James and K V Suseela (1992) Internal wave characteristics in the eastern Arabian Sea during summer monsoon. *Proceeding of the Indian Academy of Sciences*, 101, 317-327.

Murthy P G K and P N Ananth (1994) Internal waves and their diurnal activity in the coastal waters around India Symposium on Underwater systems, NSTL, Vizag

Murthy P G K and P V Hareesh Kumar (1991) Response of coastal waters off Karwar to a deep depression. *Continental Shelf Research*, 11, 239-250.

Murthy P G K and V V James (1995) Some aspects of internal waves in the coastal waters off Cochin. *Indian Journal of Marine Sciences* (in press)

Narayana Pillai V, P K Vijayarajan and A Nandakumar (1980) Oceanographic investigations off the southwest coast of India. *FAO/UNDP Report*, (FAO, Rome),pp51.

Pankajakshan T and D V Ramaraju (1987) In : Contributions in Marine Sciences. T S S Rao et al (Editors),pp237.

Phillips O M (1977) The dynamics of the upper ocean. Cambridge University Press, New York, pp336.

Pickard G L and W J Emery (1982) Descriptive Physical Oceanography. An Introduction, Pergamon Press, Oxford, pp249.

Pinkel R and J T Sherman (1991) Internal wave induced fluctuations in the oceanic density and sound speed fields. *Ocean Variability and acoustic propagation*, Potter J and A Warn-Varnas (eds) Kluwer Publishers, Netherlands, 103-118.

Pollard R T (1970) On the generation by wind of internal waves in the ocean. *Deep Sea research*, 17, 795-812.

Pond S Pickard G L (1983) Introductory Dynamical oceanography Pergamon Press, Newyork, pp321.

Porter R P, R C Spindel and R J Jafee (1974) Acoustic internal wave interaction at long ranges in the ocean. *Journal of Acoustical Society of America*, 56, 1424-1436.

Prasannakumar S, M T Babu and Ramanamurthy T V (1992) Sound speed structure and propagational characteristics of a cold core eddy in the Bay of Bengal. *Physical Processes in the INDIAN SEAS proceedings, ISPSO*, 1990, 51-55.

Prasannakumar S, T V Ramana Murthy, R K Somayajulu, P V Chodankar and C S Murthy (1994) Reference sound speed profile and related ray Acoustics of Bay of Bengal for tomographic studies. *Acoustics*, 80, 127-137.

Quadfasel D R and F Schott (1982) Watermass distribution at intermediate layers off the Somali Coast during the southwest monsoon 1979. *Journal of Physical Oceanography*, 12, 1358-1372.

Quadfasel D R and F Schott (1983) Southward subsurface flow below the Somali current. *Journal of Geophysical Research*, 88, 5973

Ramana Murthy T V, Y K Somayajalu, P V Chodankar and C S Murthy (1993) Acoustic characteristics of the waters of the Bay of Bengal. *Indian Journal of Marine Sciences*, 22, 263-267.

Ramesh Babu V and J S Sastry (1984) Summer cooling in the east central Arabian Sea - A process of dynamic response to the southwest monsoon. *Mausam*, 35, 17-26.

Rao D P, R V N Sarma, J S Sastry and K Premchand (1976) On the lowering of the sea surface temperature in the Arabian Sea with the advance of southwest monsoon. Proceeding of the symposium on *Tropical Monsoons* (Indian Institute of Tropical Meteorology, Pune) 106-115.

Rao R R (1986) Cooling and deepening of the mixed layer in the central Arabian Sea during MONSOON-77 : Observations and simulations. *Deep-Sea Research*, 33, 1413-1424.

Rao R R (1987) The observed variability of the cooling and deepening of the mixed layer in the central Arabian Sea during monsoon-77. *Mausam*, 38, 43-48.

Rao R R and B Mathew (1990) A case study on the mixed layer variability in the south central Arabian Sea during the onset phase of MONEX-79. *Deep-Sea Research*, 37, 227-243.

Rao R R, B Mathew and P V Hareesh Kumar (1993) A summary of results on thermohaline variability in the upper layers of the east central Arabian Sea and Bay of Bengal during summer monsoon experiments. *Deep Sea Research*, 40, 1647-1672.

Rao R R, P V Hareesh Kumar and B Mathew (1990) Watermass modification in the upper layers of the Arabian Sea during ISMEX-73. *Mausam*, 41, 611-620.

Rao R R, R L Molinari and J F Festa (1989) Evolution of the Climatological Near-Surface Thermal Structure of the Tropical Indian Ocean I : Description of Mean Monthly Mixed Layer Depth, Sea Surface Temperature, Surface Current and Surface Meteorological Fields. *Journal of Geophysical Research*, 94, 10801-10815.

Rao R R, R L Molinari and J F Festa (1991) Surface meteorological and near surface oceanographic Atlas of the tropical Indian Ocean. (NOAA Technical Memorandum, ERL AOML-69) pp59.

Rao Tatavarti, N Mohan Kumar and P V Hareesh Kumar (1995) Mixing processes and internal waves on the continental shelf off Cochin. *Indian Journal of Marine Sciences* (in press)

Reverdin G (1987) The upper equatorial Indian Ocean : The climatological seasonal cycle. *Journal of Physical Oceanography*, 17, 903-927.

Robinson A R(1983) Overview and summery of Eddy science. *Eddies in Marine Sciences* (Ed.by Robinson A R) Springer-Verlag, Berlin Heidelberg. pp609.

Robinson M K, R A Baur and E H Schroeder (1979) Atlas of North Atlantic-Indian Ocean monthly mean temperature and mean salinities of the surface layer. (Naval Oceanographic Office, Washington DC) pp213.

Rochford D J (1964) Salinity maxima in the upper 1000m of the north Indian Ocean. *Australian Journal of Marine and Freshwater Research*, 15, 1-24.

Rubestein D and M H Brill (1991) Acoustic variability due to internal waves and surfaces waves in shallow water.*Ocean variability and acoustic propagation*, J Potter and A Warn-Varnas (eds) Kluwer Academic Publishers, Netherlands, 215-228.

Saha K R (1974) Some aspects of the Arabian Sea summer monsoon. *Tellus*, 26, 464-476.

Sastry J S and R S D'Souza (1970) Oceanography of the Arabian Sea during southwest monsoon season - Part I : Thermal structure. *Indian Journal of meteorology and Geophysics*, 21, 367-382.

Sastry J S and R S D'Souza (1971) Oceanography of the Arabian Sea during southwest monsoon season - Part II : Stratification and Circulation. *Indian Journal of Meteorology and Geophysics*, 22, 23-34.

Sastry J S and R S D'Souza (1972) Oceanography of the Arabian Sea during southwest monsoon season - Part III : Salinity. *Indian Journal of Meteorology and Geophysics*, 23, 479-490.

Sastry J S and V Ramesh Babu (1979) Convergence of Ekman wind driven layer and surface circulation in the Arabian Sea during southwest monsoon. *Mahasagar*, 12, 201-211.

Schott F (1983) Monsoon response of the Somali Current and associated upwelling. *Progress in Oceanography*, 12, 357-381.

Schott F and D R Quadfasel (1982) Variability of the Somali current system during the Onset of the South west Monsoon.12, 1343-1357.

Schott F and D R Quadfasel (1983) Variability of Somali current system during the onset of southwest monsoon of 1979. *Journal of Physical Oceanography*, 12, 1343-1357.

Sharma G S (1966) Thermocline as an indicator of upwelling. *Journal of Marine Biological Association India*, 3, 8-19.

Sharma G S (1968) Seasonal variation of some hydrographic properties of the shelf water off the west coast of India. *Bulletin of the National Institute of Sciences*, 38, 263-275.

Sharma G S (1976) Transequatorial movement of watermasses in the Indian Ocean. *Journal of Marine Research*, 34, 143-154.

Sharma G S (1978) Upwelling off the southwest coast of India. *Indian Journal of Marine Sciences*, 7, 207-218.

Shenoi S S C and M K Antony (1991) Current measurements over western continental shelf of India. *Continental Shelf Research*, 11, 81-94.

Shetye S R (1986) A model study of the seasonal cycle of the Arabian Sea surface temperature. *Journal of Marine Research*, 44, 521-542.

Shetye S R, A D Gouveia, S S C Shenoi, D sundar, G S Michael, A M Almeida and K Santanam (1990) Hydrography and Circulation off the west coast of India during the Southwest Monsoon 1987. *Journal of Marine Research*, 48, 359-378.

Shetye S R, S S C Shenoi and D Sundar (1991) Observed low frequency currents in the deep mid-Arabian Sea. *Deep Sea Research*, 38, 57-65.

Sikka D R and R Grossman (1980) Summer MONEX Chronological weather summary. *International MONEX management Center, New Delhi*

Smith R L and J S Bottero (1977). On upwelling in the Arabian Sea. In : A voyage of Discovery, M Angel (Ed.), Pergamon Press, 291-304.

Somayajalu Y K, T V R Murthy, S P Kumar and C S Murthy (1994) Simulation studies related to acoustic propagation in the Arabian Sea. *Acoustic Letters*, 17, 173-183.

Stanford G,(1974) Low frequency fluctuations of a CW signal in the Ocean, *Journal of Acoustical Society of America*,55,968-976.

Swallow J C(1983) Eddies in Indian Ocean, Eddies in marine sicence (ed by AR Robinson) Springer-Verlag Berlin Heidelberg 200-218.

Swallow J C (1984) Some aspects of physical oceanography of the Indian Ocean. *Deep Sea Research*, 31, 639-650.

Swallow J C and J G Bruce (1966) Current measurements off the Somali Coast during the southwest monsoon in 1964. *Deep-Sea Research*, 13, 861-888.

Swallow J C, R L Molinari, J G Bruce, O B Brown and R H Evans (1983) Development of near surface flow pattern and watermass distribution in the Somali Basin in response to the southwest monsoon of 1979.*Journal of Physical Oceanography*, 13, 1398-1415.

Taft B A and J A Knauss (1967) The Equatorial Undercurrent of the Indian Ocean as observed by the Lusiad expedition. *Bulletin of Scripps Institution of Oceanography*, 9, pp 163.

Unni S and C Kaufman(1981) Acoustic fluctuations due to the temperature fine structure of the ocean. *Journal of Acoustical Society of America* 69(3) 676-680.

Urick R J (1982) Sound Propagation in the Sea, Peninsula Publisher, California pp215.

Urick R J (1983) Principles of Underwater sound McGraw-Hill Book Company, New York .pp423.

Varkey M J (1980) Power spectra of currents off Bombay. *Indian Journal of Marine Sciences*, 9, 278-280.

Vastanov A C and G E Owens (1973) On the acoustic characteristics of a gulf stream cyclonic ring. *Journal of Physical Oceanography*, 3, 470-478.

Warren B, H Stommel and J C Swallow (1966) Watermasses and patterns of flow in the Somali Basin during the southwest monsoon of 1964. *Deep-Sea Research*, 13, 825-860.

Weinberg N L and J G Clark (1980) Horizontal acoustic refraction through ocean mesoscale eddies and fronts. *Journal of Acoustical Society of America*, 68, 703-706.

Weinberg L and X Zabalagogeazcoa (1977) Coherent ray propagation through a Gulf Stream. *Journal of Acoustical Society of America*, 62, 888-894.

Wilson W D (1960) Equation for the speed of sound in Sea water . *Journal of Acoustical Society of America* 32 1357

Wyrtki K (1964) Thermal structure of the Eastern Pacific Ocean. Deutsche Hydr.Zeit.,Erganzungsheft Reihe A(8°),Nr.6. Hamburg.

Wyrtki K (1971) Oceanographic Atlas of the International Indian Ocean Expedition (US Government Printing Office, Washington DC) pp531.

Wyrtki K (1973) An equatorial Jet in the Indian Ocean. *Science*, 11, 262-264.

Yoshida K and H L Mao (1957) A theory of upwelling of large horizontal extent. *Journal of Marine Research*, 16, 40-54.